ELSEVIER

Journal of Molecular Structure 441 (1998) 39–46

Journal of
MOLECULAR
STRUCTURE

Cationic motions and crystal structures of 1,3,5-trimethylpyridinium hexachlorometallates $[(CH_3)_2C_5H_3N(CH_3)]_2MCl_6$ (M is Sn and Te) studied by ^1H NMR and X-ray diffraction

Setsuko Sato[a,*], Hiroyuki Ishida[b], Makoto Nagae[a], Setsuo Kashino[b], Yoshihiro Furukawa[c], Alarich Weiss[1,d]

[a]Department of Chemistry, Faculty of Education, Gifu University, Gifu 501-11, Japan
[b]Department of Chemistry, Faculty of Science, Okayama University, Okayama 700, Japan
[c]Faculty of School Education, Hiroshima University, Higashi-Hiroshima 739, Japan
[d]Institut für Physikalische Chemie III, Technische Hochschule Darmstadt, D-64285 Darmstadt, Germany

Received 10 June 1997; accepted 15 July 1997

Abstract

The crystal structure of 1,3,5-trimethylpyridinium hexachlorometallates $[(CH_3)_2C_5H_3N(CH_3)]_2MCl_6$ (M is Sn and Te) were determined at 298 K and found to be orthorhombic Pnnm (No. 58) and $Z = 2$, $a = 8.996(2)$, $b = 11.330(2)$, $c = 11.596(2)$ Å, $V = 1182.0(7)$ Å^3 for the stannate, and $a = 9.072(4)$, $b = 11.399(5)$, $c = 11.63(2)$ Å, $V = 1203(3)$ Å^3 for the tellurate, by single-crystal X-ray diffraction. No phase transition was detected by DTA from 80 to 573 K. The cationic motions were studied by ^1H NMR and the C_3 reorientation of the CH_3 groups was observed below 273 K, having an activation energy of 3.1 kJ mol^{-1} for the stannate and 3.7 kJ mol^{-1} for the tellurate. Another cationic motion, with an activation energy of about 20 kJ mol^{-1}, was observed above 380 K for both salts. This is attributable to the pseudo-C_3 reorientation around the axis perpendicular to the pyridinium ring. The cationic motions and the crystal structure are discussed from the point of view of the hydrogen bonding.

Keywords: Molecular dynamics; Crystal structure spectroscopy; Nuclear magnetic resonance

1. Introduction

Many hexahalometallates A_2MX_6, with spherical cations such as alkali metal and ammonium ions, have been studied by NQR and NMR with respect to the highly symmetric crystal structure of K_2PtCl_6 type [1–6]. For complex salts with partially methyl-substituted ammonium ions such as $(CH_3)_nNH_{4-n}$ (n = 1–3), the phase transitions are of interest in view of the hydrogen bonds –H–H···X and of the ionic motions which are inhibited by the hydrogen bonds [7–12].

For $(CH^3NH_3)_2MX_6$ (M is Sn, Pb, Pd, Pt, and Se; X is Cl, Br, and I), the crystal structures have been reported to be isomorphous, displaying the rhombohedral system (R3m) at room temperature [7]. In these structures, the cations were found to perform the C_3 reorientation around the C–N bond axis and no overall rotation [8]. It was also revealed that in the stannate

* Corresponding author.
[1] Deceased.

0022-2860/98/$19.00
PII S0022-2860(97)00281-0

Table 1
Experimental conditions for the crystal determination and crystallographic data for $[(CH_3)_2C_5H_3N(CH_3)]_xMCl_6$ (M is Sn and Te) at 298 K

Diffractometer	Rigaku AFC-5R	
Radiation and wavelength/Å	Mo Kα = 0.71073	
Scan	$\omega/2\theta$	
$2\theta_{max}$/°	55.0	
No. of reflections for cell determination	25 (2θ = 22–23°)	
	Sn	Te
T/K	298	298
Crystal colour, habit, and size/mm	Brown, prismatic 0.15 × 0.15 × 0.30	Yellow, prismatic 0.15 × 0.10 × 0.25
Crystal system	Orthorhombic	Orthorhombic
Absorption coef./mm^{-1}	1.761	1.915
No. of measured reflections	1772	1806
No. of unique reflections	1586(R_{int} = 0.017)	1616(R_{int} = 0.029)
No. of observed reflections	817 [$I > 3\sigma(I)$]	605[$I > 3\sigma(I)$]
No. of parameters	66	66
Space group	Pnnm (No. 58)	Pnnm (No. 58)
Lattice constants a/Å	8.996(2)	9.072(4)
b/Å	11.330(2)	11.399(5)
c/Å	11.596(2)	11.63(2)
Volume of the unit cell, V/Å^3	1182.0(7)	1203(3)
Formula units per unit cell, Z	2	2
D_{calc}/Mg m^{-3}	1.618	1.614
R	0.046	0.047
wR	0.046	0.039

the three H atoms are engaged in trifurcated N–H···Cl bonds at room temperature, which form two-dimensional networks among the ions [9]. However, for $(CH_3NH_3)_2TeX_6$ (X is Br and I), the crystal structures were determined to be isomorphous with K_2PtCl_6 ($Fm\bar{3}m$) and the cation performs the overall rotation [10].

For $[(CH_3)_2NH_2]_2MCl_6$ (M is Sn and Te), it has been reported that the cation performs the C_3 reorientation of the CH_3 groups and the 180° flip motion around the pseudo-C_2 axis in an orthorhombic structure (Pmnn) [11] and that two H atoms have trifurcated N–H···Cl bonds which form one-dimensional networks of $SnCl_6$···NH_2···$SnCl_6$ [9].

For $[(CH_3)_3NH]_2SnCl_6$, it has been shown that the cationic C_3 reorientation around the N–H bond occurs in addition to the CH_3 C_3 reorientation in the crystal which forms a cubic lattice ($Pa\bar{3}$) [12]. It was suggested that the H atom is engaged in symmetrically trifurcated N–H···Cl bonds [9].

In summary, it seems that the hydrogen bonding networks inhibit the overall cationic rotation and make the symmetry of a crystal structure lower. In the case of $(CH_3NH_3)_2TeX_6$ (X is Br and I), it is considered that the TeX_6 octahedron is much larger than the other MX_6 (M is Sn, Pb, Pd, Pt, and Se; X is Cl, Br, and I) and it gives sufficient space for the cation to perform the overall rotation.

As examples of large cations of low symmetry, $(C_5H_5NH)_2MCl_6$ (M is Sn, Te, and Pb) were studied [13]. There it was revealed that the N–H hydrogen atom is connected by trifurcated hydrogen bonds to two neighbouring MCl_6 octahedra in the triclinic lattice (P1). Here we study the cationic motions and the crystal structures of $[(CH_3)_2C_5H_3N(CH_3)]_2MCl_6$ (M is Sn and Te) in which no hydrogen bond is expected.

2. Experimental

1,3,5-Trimethylpyridinium iodine synthesized from 3,5-lutidine and methyl iodide was mixed with silver oxide to obtain 1,3,5-trimethylpyridinium hydoxide.

Then, 1,3,5-trimethylpyridinium hexachlorostannate ($(TMPy)_2SnCl_6$) and -tellurate ($(TMPy)_2TeCl_6$) were prepared by mixing the hydroxide with tin(IV) chloride and tellurium(IV) oxide, respectively, in hydrochloric acid. Purification was made by recrystallization in hydrochloric acid. Analysis: calcd. for $(TMPy)_2SnCl_6$: C, 33.4; H, 4.2%; found: C, 33.3; H, 4.3%. Calcd. for $(TMPy)_2$ $TeCl_6$: Cl, 36.4; C, 33.9; found: Cl, 36.2; 32.6; H, 4.2%.

Single-crystal X-ray measurements were carried out at 298 K using a Rigaku AFC-5R diffractometer with graphite-monochromated Mo Kα radiation (50 kV, 200 mA). The structures were solved by direct methods using MITHRIL [14] and DIRDIF [15]. All calulations were performed on a VAX 3100 computer using TEXSAN [16]. Experimental details for structure analyses and crystal data are summarized in Table 1.

The ^{1}H NMR spin-lattice relaxation time (^{1}H T_1) was measured at 32 MHz with a 180°–τ–90° pulse sequence using a pulsed spectrometer, as already reported [17]. Wide-line ^{1}H NMR absorption spectra were recorded to evaluate the ^{1}H NMR second moment (M_2) using a JEOL JNM-MW-40S spectrometer operated at 40 MHz.

3. Results

3.1. X-ray diffraction

$(TMPy)_2SnCl_6$ and $(TMPy)_2TeCl_6$ are isostructural with each other, having the orthorhombic space group Pnnm (No. 58). The crystal structure of $(TMPy)_2SnCl_6$ is shown in Fig. 1. The Sn and Te atoms are located on the mirror plane in the crystal, and the $SnCl_6^{2-}$ and $TeCl_6^{2-}$ form slightly distorted octahedra. The plane of the pyridinium ring is perpendicular to the mirror plane. In order to determine the nitrogen position in the pyridinium ring, we considered three model structures. In the first model, the N atom is put at site 4 (Fig. 1), i.e. the crystal is in an ordered state. In the second model, the N and C atoms are disordered over sites 2 and 2′, and in the third model the N and two C atoms are disordered over sites 2, 2′, and 4. As a reference, we examined the fourth model, where all atoms are assumed to be C. These models were refined by a least-squares

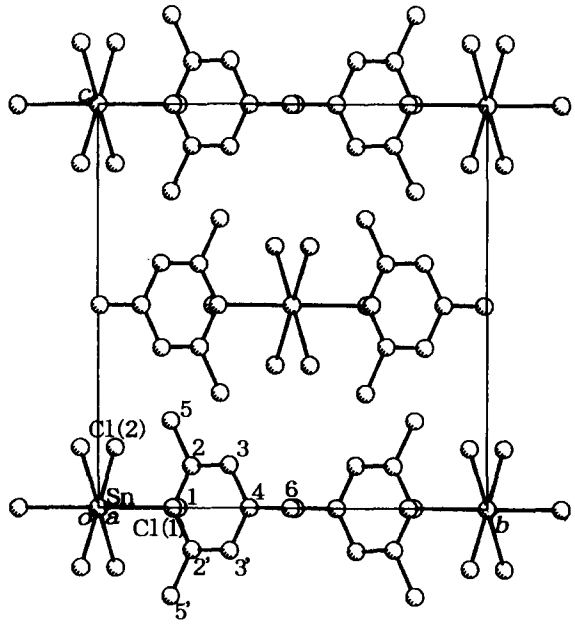

Fig. 1. Projection of the crystal structure along the *a* axis for $(TMPy)_2SnCl_6$. Because of the disordering in the TMPy ring, site numbering is used in place of atomic numbering in the ring.

method and the refinements were performed with anisotropic displacement parameters for non-hydrogen atoms. The H atoms were not included in the refinements. For the second and third models, the temperature factors of C and N occupying the same site were assumed to be the same. In addition, for the third model, the N atom was assumed to be equally populated among sites 2, 2′, and 4. The equivalent isotropic displacement parameters, B_{eq} (Å^2), obtained for sites 1–4, the bond lengths (Å) between the sites, R and weighted R (wR) factors are given in Table 2 and Table 3 for $(TMPy)_2SnCl_6$ and $(TMPy)_2TeCl_6$, respectively. The displacement parameter for site 4 in the first model is significantly larger than in the others. Moreover, for all the models the distance between sites 3 and 4 is always longer than the others. We expect that the pyridinium ring atoms have almost the same displacement parameters and the bond length of C–N is shorter than that of C–C. Therefore, it can be concluded that the N atom is not on site 4 with an occupancy of 1, but rather populates sites 2 and 2′ with a higher occupancy than site 4. This means that the crystal is in a disordered state at 298 K. Although we could not determine the occupancy

Table 2
Comparison of the four models for $[(CH_3)_2C_5H_3N(CH_3)]_2SnCl_6$

Atom site[a]	Model 1 (ordered)		Model 2 (2 sites disordered)		Model 3 (3 sites disordered)		Model 4 (all carbon)	
	Species of atom	B_{eq}/Å^{2}[b]	Species of atom	B_{eq}/Å^{2}	Species of atom	B_{eq}/Å^{2}	Species of atom	B_{eq}/Å^{2}
1	C	5.2(7)	C	5.2(7)	C	5.2(7)	C	5.2(7)
2	C	4.5(4)	C, N	5.7(4)	C, N	5.3(4)	C	4.4(4)
3	C	6.0(5)	C	6.1(5)	C	6.0(5)	C	6.0(5)
4	N	8.5(8)	C	5.6(7)	C, N	6.5(7)	C	5.6(7)
Bond length/ (Å) between								
1–2	1.374(9)		1.385(8)		1.381(8)		1.376(9)	
2–3	1.37(1)		1.403(9)		1.391(9)		1.39(1)	
3–4	1.44(1)		1.407(9)		1.420(9)		1.41(1)	
R	0.049		0.046		0.046		0.047	
wR	0.047		0.046		0.046		0.049	

[a]The numbering of the sites in the pyridinium ring is given in Fig. 1.
[b]$B_{eq} = (8\pi^2/3)\Sigma_i\Sigma_j U_{ij} a_i^* a_j^* \boldsymbol{a}_i \boldsymbol{a}_j$.

ratio of the N atom on sites 2, 2′, and 4, the second model is considered close to the real structure. The atomic parameters of $(TMPy)_2SnCl_6$ and $(TMPy)_2TeCl_6$ obtained for this model are listed in Table 4, and the intraionic bond lengths and angles, as well as the interionic distances shorter than 3.75 Å, are given in Table 5.

3.2. ^{1}H NMR measurements

The M_2 values observed for the stannate and tellurate are shown in Fig. 2 and Fig. 3, respectively. M_2 is constant at 8–9 G^2 between 77 and 425 K for the stannate and between 105 and 373 K for the tellurate. T_1 was measured from 105 to 465 K for

Table 3
Comparison of the four models for $[(CH_3)_2C_5H_3N(CH_3)]_2TeCl_6$

Atom site[a]	Model 1 (ordered)		Model 2 (2 sites disordered)		Model 3 (3 sites disordered)		Model 4 (all carbon)	
	Species of atom	B_{eq}/Å^{2}[b]	Species of atom	B_{eq}/Å^{2}	Species of atom	B_{eq}/Å^{2}	Species of atom	B_{eq}/Å^{2}
1	C	5(1)	C	5(1)	C	5(1)	C	5(1)
2	C	4.7(6)	C, N	6.0(5)	C, N	5.5(5)	C	4.5(6)
3	C	6.1(8)	C	6.0(7)	C	6.0(7)	C	6.0(8)
4	N	9(1)	C	6(1)	C, N	7(1)	C	6(1)
Bond length/ (Å) between								
1–2	1.36(1)		1.37(1)		1.37(1)		1.36(1)	
2–3	1.37(1)		1.41(1)		1.40(1)		1.39(1)	
3–4	1.45(1)		1.41(1)		1.43(1)		1.41(1)	
R	0.051		0.047		0.048		0.049	
wR	0.042		0.039		0.040		0.043	

[a]The numbering of the sites in the pyridinium ring is given in Fig. 1.
[b]$B_{eq} = (8\pi^2/3)\Sigma_i\Sigma U_{ij} a_i^* a_j^* \boldsymbol{a}_i \boldsymbol{a}_j$.

Table 4
Positional and thermal parameters of $(C_8H_{12}N)_2MCl_6$ (M is Sn and Te). The coefficients U_{ij} of the anisotropic temperature factor expression are defined as follows:exp$[-2\pi^2(a^{*2}U_{11}h^2+b^{*2}U_{22}k^2+c^{*2}U_{33}l^2+2a^*b^*U_{12}hk+2a^*c^*U_{13}hl+2b^*c^*U_{23}kl)]$

Atom	[Site]	x	y	z	U_{11}	U_{22}	U_{33}	U_{12}	U_{13}	U_{23}
Sn		0	0	0	0.0481(6)	0.0435(6)	0.0865(9)	−0.0033(7)	0	0
Cl(1)		0.0802(3)	0.2039(2)	0	0.080(2)	0.049(2)	0.116(3)	−0.014(2)	0	0
Cl(2)		−0.1823(2)	0.0442(2)	0.1474(2)	0.083(2)	0.072(1)	0.128(2)	0.001(1)	0.036(2)	−0.002(1)
C(1)	[1]	0.470(1)	0.189(1)	0	0.05(1)	0.057(7)	0.09(1)	0.014(6)	0	0
C(2), N	[2]	0.5140(8)	0.2400(5)	0.1030(7)	0.052(4)	0.054(4)	0.109(6)	−0.010(4)	0.006(6)	−0.007(4)
C(3)	[3]	0.6072(8)	0.3393(7)	0.1046(8)	0.045(4)	0.054(5)	0.131(9)	0.003(4)	−0.002(6)	−0.011(5)
C(4)	[4]	0.655(1)	0.390(1)	0	0.042(7)	0.058(7)	0.11(1)	−0.001(6)	0	0
C(5)	[5]	0.463(1)	0.1858(7)	0.2167(7)	0.100(8)	0.093(6)	0.071(6)	−0.012(5)	0.019(6)	0.011(5)
C(6)	[6]	0.758(1)	0.495(1)	0	0.087(9)	0.080(8)	0.15(1)	−0.049(8)	0	0
Te		0	0	0	0.0483(8)	0.0397(7)	0.096(1)	−0.004(1)	0	0
Cl(1)		0.0827(4)	0.2119(3)	0	0.091(3)	0.049(2)	0.135(4)	−0.016(2)	0	0
Cl(2)		−0.1886(3)	0.0452(2)	0.1533(3)	0.091(2)	0.070(2)	0.150(3)	0.002(2)	0.044(2)	−0.002(2)
C(1)	[1]	0.469(2)	0.192(1)	0	0.05(1)	0.044(8)	0.09(1)	0.006(8)	0	0
C(2), N	[2]	0.510(1)	0.2392(7)	0.104(1)	0.055(6)	0.048(5)	0.12(1)	0.009(7)	0.00(1)	−0.018(6)
C(3)	[3]	0.606(1)	0.3368(9)	0.104(1)	0.047(7)	0.052(7)	0.13(1)	0.005(6)	−0.004(8)	−0.008(8)
C(4)	[4]	0.653(2)	0.387(1)	0	0.06(1)	0.06(1)	0.12(2)	0.001(8)	0	0
C(5)	[5]	0.461(1)	0.1860(8)	0.2157(9)	0.10(1)	0.089(7)	0.065(8)	−0.013(7)	0.026(8)	0.017(7)
C(6)	[6]	0.758(2)	0.492(2)	0	0.08(1)	0.08(1)	0.16(2)	−0.06(1)	0	0

Table 5
Intra- and interionic bond lengths (Å) and angles (°) of $(TMPy)_2MCl_6$ (M is Sn and Te)

M	Sn	Te
M–Cl(1)	2.420(3)	2.530(4)
M–Cl(2)	2.422(2)	2.525(4)
N(2)–C(1)	1.385(8)	1.37(1)
N(2)–C(3)	1.403(9)	1.41(1)
N(2)–C(5)	1.52(1)	1.50(1)
C(3)–C(4)	1.407(9)	1.41(1)
C(4)–C(6)	1.51(1)	1.53(1)
Cl(1)–M–Cl(2)	90.26(7)	90.29(9)
Cl(1)–M–Cl(2)	89.74(7)	89.71(9)
Cl(2)–M–Cl(2)	90.2(1)	90.1(2)
Cl(2)–M–Cl(2)	89.8(1)	89.9(2)
C(1)–N(2)–C(3)	121.1(8)	119(1)
C(1)–N(2)–C(5)	119.5(6)	121.7(9)
C(3)–N(2)–C(5)	119.4(7)	120(1)
N(2)–C(1)–N(2)	119(1)	123(1)
N(2)–C(3)–C(4)	119.7(9)	120(1)
C(3)–C4)–C(6)	119(1)	120.5(7)
Interionic		
Cl(1)···C(1)	3.51(1)	3.51(2)
Cl(1)···C(5)	3.669(8)	3.68(1)
Cl(2)···N(2)	3.557(7)	3.56(1)
Cl(2)···C(5)	3.658(8)	3.63(1)

the stannate and from 105 to 480 K for the tellurate as shown in Fig. 4 and Fig. 5. For both complex salts, T_1 decreases with decreasing temperature below 273 K. This decrease gives an activation energy (E_a) of 3.1 kJ mol^{-1} to cationic motion in the stannate and of 3.7 kJ mol^{-1} in the tellurate, by assuming the Arrhenius equation for the correlation time (τ_c) of the motion:

$$\tau_C = \tau_0 \exp\left(\frac{E_a}{RT}\right)$$

Similarly, the T_1 decrease with increasing temperature above 400 K indicates that another cationic motion

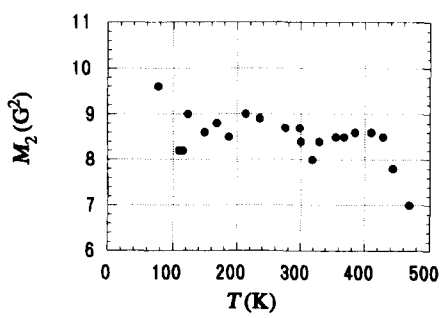

Fig. 2. Temperature dependence of the ^{1}H NMR absorption second moment M_2 of $(TMPy)_2SnCl_6$.

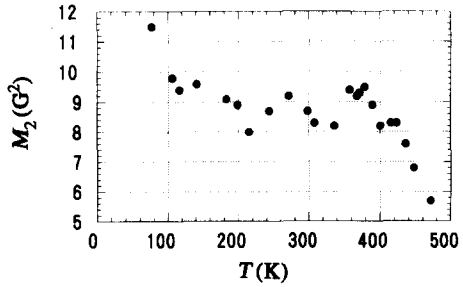

Fig. 3. Temperature dependence of the ^{1}H NMR absorption second moment M_2 of $(TMPy)_2TeCl_6$.

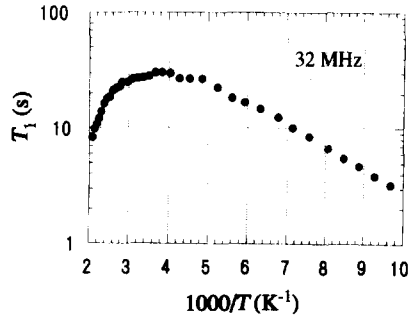

Fig. 5. Temperature dependence of the ^{1}H NMR spin-lattice relaxation time T_1 at 32 MHz for $(TMPy)_2TeCl_6$.

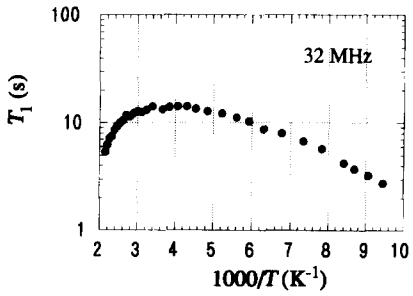

Fig. 4. Temperature dependence of the ^{1}H NMR spin-lattice relaxation time T_1 at 32 MHz for $(TMPy)_2SnCl_6$.

exists and is accelerated with increasing temperature at an E_a of about 20 kJ mol^{-1} in both salts.

3.3. DTA and NQR measurements

The differential thermal analysis (DTA) was carried out from 80 to 573 K using a home-made apparatus [7] and no heat anomaly was observed for either complex salt.

The NQR measurement was performed at room and liquid N_2 temperatures using a pulsed NQR spectrometer [18] for the stannate and a super-regenerative spectrometer [1] for the tellurate. No signal was detected for either complex salt.

4. Discussion

The theoretical M_2 values were calculated for the cationic structure determined for the tellurate by X-ray diffraction, assuming 1.08 Å for the pyridinium ring C–H bond length and 1.09 Å for the CH_3 C–H bond length. The three protons of a CH_3 group are assumed to be at the centre of a triangle consisting of the protons, in order to estimate the contribution of CH_3–H and CH_3–CH_3. These calculated M_2 values are given in Table 6. The value of 8.0 G^2 assuming CH_3 C_3 reorientation agrees very well with the experimental value of 8–9 G^2. Hence we conclude that all CH_3 groups perform C_3 reorientation above 77 K for the stannate and above 100 K for the tellurate. When the T_1 results are compared with these facts, it is clear that the E_a value of 3.1 kJ mol^{-1} is assigned to the CH_3 C_3 reorientation in the stannate and 3.7 kJ mol^{-1} to that in the tellurate.

M_2 decreases with increasing temperature again above 380 K for the tellurate and above 420 K for the stannate. This means that another cationic motion

Table 6
Calculated second moment values (M_2/G^2) of ^{1}H NMR absorptions for $(TMPy)_2TeCl_6$. The distances between the protons of inter-CH_3 and CH_3–H were calculated by assuming the three protons in CH_3 are placed at the centre of a triangle consisting of the three protons

	Intra-CH_3	CH_3–H	Inter-CH_3H-H	Interion	Sum
Rigid lattice	16.9	> 1.6	> 0.1	> 2.0	> 21
CH_3 C_3 reorientation	4.2	1.6	0.1	2.0	8
CH_3 C_3 and C_2 reorientations	2.9	1.1		< 2.0	< 6
CH_3 C_3 and pseudo-C_3 reorientations	1.1	0.4		< 2.0	< 3.5

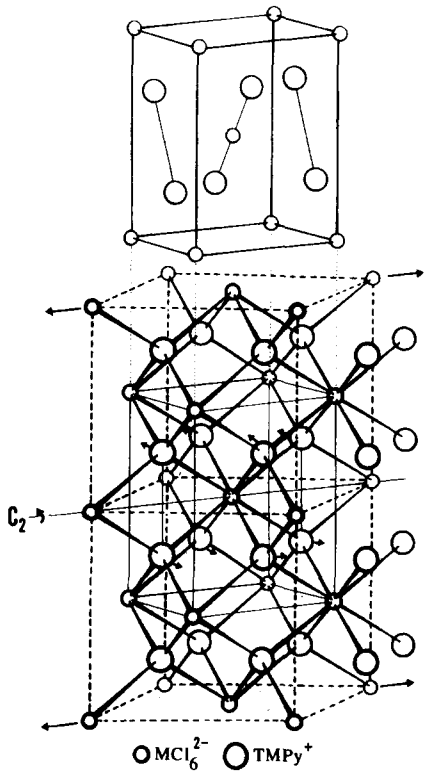

Fig. 6. The structure of $(TMPy)_2MCl_6$ (M is Sn and Te) modified by expanding the K_2PtCl_6 type $Fm\bar{3}m$ unit cell diagonally as shown by arrows and then by rotating the TMPy ions slightly along the C_2 axis.

occurs above these temperatures for both complex salts. From the X-ray diffraction at 298 K, trimethylpyridinium cations are disordered, the N atom populating sites 2 and 2′ with high occupancy. Therefore, the above cationic motion may be a pseudo-C_3 reorientation around the axis normal to the pyridinium ring, or a C_2 reorientation around the C_2 axis on which sites 1, 4, and 6 lie. Since reduction of M_2 by the pseudo-C_3 reorientation or the C_2 reorientation was not observed at room temperature, the rate of the reorientation must be less than 10^4–10^5 Hz at room temperature and the decrease of M_2 at around 400 K results from the accelaration of the reorientation, having an E_a of approx. 20 kJ mol^{-1}. This E_a value is not large enough to consider the motion as the C_2 reorientation. Because the pyridinium rings are stacked along the a axis, whose lattice constant of 9.072 Å is much shorter than the 11.399 Å for b and 11.63 Å for c, the C_2 reorientation is expected to be hindered considerably. Therefore, we expect that the cationic motion is the pseudo-C_3 reorientation whose potential wells might be unequal for the states in which the N atom is placed on site 2 (or 2′) and site 4. From the atomic positions determined by X-ray diffraction for the second model, we estimated the shortest H(C(5))···Cl(2) distances to be 2.60 Å between the cation and the anion lying on the same mirror plane, and 2.62 Å between the same CH_3 and the other $TeCl_6$ related to the original $TeCl_6$ by a two-fold screw rotation. These distances are shorter than 3.0 Å, the sum of the van der Waals radii for H and Cl atoms. The E_a values of the CH_3 C_3 reorientation for both salts are quite small. Therefore, we believe that the methyl protons whose C atom is bonded to the N atom in the pyridinium ring take part in weak hydrogen bonding. This kind of hydrogen bonding has been reported in a number of salts [19].

In the case of $[(CH_3)_2NH_2]_2SnCl_6$, it has been reported that the hydrogen bond makes one-dimensional networks of $SnCl_6$···NH_2···$SnCl_6$. In $(C_5H_5NH)_2SnCl_6$, each pyridinium cation is connected to two neighbouring $SnCl_6$ octahedra by trifurcated hydrogen bonds in the low temperature phase of $P\bar{1}$. In the high temperature phase of B2/m known for the tellurate, C and N and two pairs of C atoms are equivalent respectively by a mirror plane perpendicular to the pyridinium ring. Hence it has been suggested that some cationic motion around the pseudo-C_6 axis of the ring averages the hydrogen bond interaction and causes the phase transition from $P\bar{1}$ to B2/m. Similarly, in $(TMPy)_2MCl_6$ (M is Sn and Te), it seems that each pyridinium cation is connected to two neighbouring MCl_6 octahedra. Even so, these hydrogen bonds alternate between the site 2 side and site 2′ side with the cationic motion, and this does not induce any phase transition between 80 and 573 K.

Referring to the structure of $[(CH_3)_2NH_2]_2SnCl_6$ [9], we can construct the unit cell of $(TMPy)_2SnCl_6$ with the face-centred $SnCl_6^{2-}$ ions placed in the distorted $Fm\bar{3}m$ structure and the cations that rotate slightly along the C_2 axis, as shown in Fig. 6.

Acknowledgements

The authors are grateful for the use of the X-ray diffractometers (Rigaku AFC-5R and Rigaku Rint-1000) in the X-ray Laboratory of Okayama University.

References

[1] D. Nakamura, Y. Kurita, K. Ito, M. Kubo, J. Am. Chem. Soc. 82 (1960) 5783.
[2] K. Ito, D. Nakamura, Y. Kurita, K. Ito, M. Kubo, J. Am. Chem. Soc. 83 (1961) 4526.
[3] D. Nakamura, M. Kubo, J. Phys. Chem. 68 (1964) 2986.
[4] L.S. Prabhumirashi, R. Ikeda, D. Nakamura, Ber. Bunsenges. Phys. Chem. 85 (1981) 1142.
[5] Y. Furukawa, L.S. Prabhumirashi, R. Ikeda, D. Nakamura, Bull. Chem. Soc. Jpn. 55 (1982) 995.
[6] S. Sato, R. Ikeda, D. Nakamura, Ber. Bunsenges. Phys. Chem. 86 (1982) 936.
[7] Y. Kume, R. Ikeda, D. Nakamura, J. Magn. Reson. 33 (1979) 331.
[8] R. Ikeda, Y. Kume, D. Nakamura, Y. Furukawa, H. Kiriyama, J. Mag. Reson. 24 (1976) 9.
[9] O. Knop, T.S. Cameron, M.A. James, M. Falk, Can. J. Chem. 61 (1983) 1620.
[10] Y. Kume, R. Ikeda, D. Nakamura, J. Phys. Chem. 82 (1978) 1926.
[11] H. Ishida, R. Ikeda, D. Nakamura, Ber. Bunsenges. Phys. Chem. 88 (1984) 546.
[12] R. Ikeda, R. Kadel, A. Weiss, N. Ishida, D. Nakamura, Ber. Bunsenges. Phys. Chem. 86 (1982) 685.
[13] D. Borchers, A. Weiss, Z. Naturforsch. 42a (1987) 739.
[14] C.J. Gilmore, J. Appl. Cryst. 17 (1984) 42.
[15] P.T. Beurskens, Direct Methods for Difference Structures, An Automatic Procedure for Phase Extention and Refinement of Difference Structure Factors. Technical Report 1984/1. Crystallography Laboratory, Toernooiveld, 6525 ED Nijmegen, The Netherlands.
[16] Molecular Structure Corporation (1985). TEXRAY Structure Analysis Package, MSC, 3200 Research Forest Drive, The Woodlands, TX77381, USA.
[17] H. Ishida, T. Iwachido, N. Hayama, R. Ikeda, M. Terashima, D. Nakamura, Z. Naturforsch. 44a (1989) 741.
[18] S. Gima, Y. Furukawa, R. Ikeda, D. Nakamura, J. Mol. Struct. 111 (1983) 189.
[19] K.M. Harmon, I. Gennick, S.L. Madeira, J. Phys. Chem. 78 (1974) 2585.